Development of catalytic materials for decomposition of ADN-based monopropellants

Corentin Maleix[1], Pierre Chabernaud, Rachid Brahmi, Romain Beauchet[2], Yann Batonneau[3], Charles Kappenstein

Institut de Chimie des Milieux et Matériaux de Poitiers (IC2MP), CNRS – UMR7285, Université de Poitiers, bât. B27, 4 rue Michel Brunet, TSA 51106, 86073 Poitiers cedex 9, France

[1]*corentin.maleix@univ-poitiers.fr*, [2]*romain.beauchet@univ-poitiers.fr*, [3]*yann.batonneau@univ-poitiers.fr*

Robert-Jan Koopmans, Sebastian Schuh, Tobias Bartok

FOTEC Forschungs- und Technologietransfer GmbH, Viktor Kaplan-Straße 2, 2700 Wiener Neustadt, Austria

Martin Schwentenwein, Manfred Spitzbart

Lithoz GmbH, Mollardgasse 85a/2/64-69, 1060 Wien, Austria

Carsten Scharlemann

Fachhochschule Wiener Neustadt, Johaness Gutenberg- Straße 3, 2700 Wiener Neustadt, Austria

Abstract

Hydrazine (N_2H_4), one of the most used liquid monopropellant is to be replaced by "greener" propellants e. g. based on ammonium dinitramide (ADN, $NH_4^+N(NO_2)_2^-$), such as LMP-103S and FLP-106 within the framework of the Horizon 2020 Rheform project. While hydrazine can rely on a catalytic technology based on conventional materials such as γ-Al_2O_3 (due to the adiabatic decomposition temperature of about 900-1 000 °C), LMP-103S and FLP-106 require catalyst support materials able to withstand higher temperatures (about 1 600 °C and 1 900 °C, respectively) and exhibit a sufficient porosity and resistance to sintering. In this paper, among the various candidates, catalysts prepared from monolith supports are investigated regarding their ability to promote both LMP-103S and FLP-106 decomposition.

1. Introduction

Hydrazine has been widely used in the world as a monopropellant, particularly after WWII [1]. Numerous catalysts based on iridium impregnated on γ-Al_2O_3 were developed to achieve spontaneous decomposition of hydrazine (Shell 405, Cnesro, KC12GA, etc.). Catalytic ignition systems are quite simple, requiring a tank, a flow control valve and an injector to work properly, and offers the advantage to be reusable. Despite its presence in the list of Substances of Very High Concern (SVHC) since 2011, hydrazine and its derivatives remain the most used propellants for spacecraft [2]. Therefore, numerous efforts have been made in order to find candidates that can substitute hydrazine. Nitrogen-rich ionic liquids are among the most promising candidates and are the subject of extensive research [3]. The advantages that these ionic liquids have over hydrazine are represented by a higher specific and volumetric impulse. Since they are likely to be non-toxic or less toxic than hydrazine, their handling cost is much lower. Ammonium DiNitramide (ADN) was selected within the framework of the Horizon H2020 Rheform project in the form of two liquid propellants blends, namely FLP-106, developed by the Swedish Defence Research Agency (FOI) and LMP-103S, developed by ECAPS [4]. Those two blends contain ADN, water, a fuel and a stabilizer for LMP-103S [5]. The current technology, a 1 N class High Performance Green Propulsion (HPGP) thruster commercialized by ECAPS has been flight-proven, reaching a TRL of 7 in 2011 [6]. It relies on LMP-103S as monopropellant and a patented hexaaluminate catalyst as ignition system. However, unlike hydrazine, which is capable of cold spontaneous decomposition, the current thruster has to be preheated up to 350 °C, for 30 min before firing [6], due to the high content of water that has to be vaporized. Several catalysts shapes were investigated in the project: (i) granulated catalysts and (ii) monolithic catalysts. Last ones present the advantage to be resistant to abrasion and not to present any preferential propellant pathways that can appear in granulated catalytic bed. A recent technologic breakthrough made by the Lithoz [7] has made the 3D printing of ceramic structures possible. Thus, complex 3D structures, impossible to obtain by conventional monolith extrusion were created and have been studied towards a washcoating process. The washcoat synthesis was carried out by a sol-gel technique adapted from the method developed by Nijhuis *et al*. [8]. A silicon-doped alumina was prepared to tentatively delay the gamma to alpha allotropic phase transition of alumina in the harsh working conditions and in this way to keep a sufficiently large specific surface area. The quality of the porous layer was inspected using Scanning Electron Microscopy (SEM) and nitrogen sorptiometry. The potential of this material as a coating layer in the catalyst was assessed by

decomposition tests with FLP-106 and LMP-103S after impregnation with solutions of active phase metallic precursor [9][10], known to ignite binary mixture of ADN/H_2O at temperature lower than the one of thermal decomposition. Finally, textural behaviour of the washcoat layer was studied after several heat treatments up to 1600 °C for different durations, to tentatively approach the harsh decomposition conditions in the thruster.

2. Experimental

2.1. Monolithic support and washcoat material

All the monoliths were produced by additive layer manufacturing (ALM), using a slurry composed of a photocurable monomer and a fine ceramic powder. Four base materials were investigated: α-alumina (α-Al_2O_3), cordierite (($MgFe)_2Al_4Si_5O_{18}$), magnesia (MgO) and silicon nitride (Si_3N_4). Their different designs are summarized in Table 1, and an example of a monolith is shown in Figure 1. A more detailed view of the cellular and polyhedral structures is presented in Figure 2.
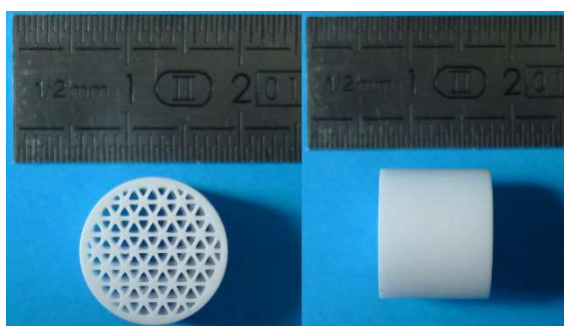

Figure 1. Overview of alumina monoliths with triangular linear channels

Table 1. Design variations of the 3D-printed monoliths

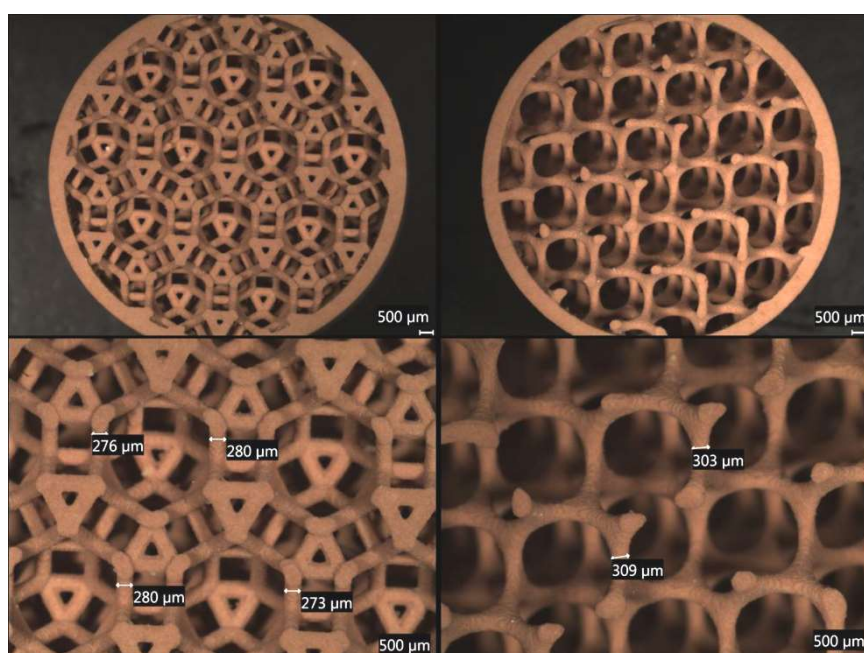| Monolith chemical nature	Geometry			
	Triangular linear channel	Cellular	Polyhedral	Diamond
α-Alumina	X			
Cordierite	X	X	X	
Magnesia	X	X	X	X
Silicon nitride	X			

Figure 2. Detailed view of the polyhedral structure (left) and cellular structure (right) of a cordierite monolith

Geometrical parameters are gathered in Table 2. CPSI in the last column of the column corresponds to the channel density per square inch.

Table 2. Monolith geometrical parameters

Monolith	Mean length ± 0.1 (mm)	Mean diameter ± 0.1 (mm)	Mean ext. wall thickness ± 0.1 (mm)	Mean internal wall thickness[a] ± 0.1 (mm)	Mean channel side[a] ± 0.1 (mm)	CPSI[a,b]
α-Alumina	10.2	12.1	0.6	0.4	1.0	760
Cordierite	10.5	12.2	0.5	0.3	1.1	760
Magnesia	10.1	12.0	0.5	0.3	1.1	760
Silicon nitride	10.0[c]	12.3[c]	0.6	0.4	1.0	760

[a]Only for monoliths with triangular linear geometry. Parameters for other geometries are shown in Figure 2
[b]Calculated according to CPSI = $(4/\sqrt{3})/$(channel side +internal wall thickness)^2, derived from [11]

2.1.1. Washcoat preparation

Preparation of the silicon-doped alumina was carried out at room temperature starting from Disperal® P2 (Sasol Company) as alumina precursor and urea (BioReagent ≥ 98 %, Sigma Aldrich) dispersed in nitric acid (ACS reagent, Sigma Aldrich) as a 0.3 mol L^{-1} solution prepared in ultrapure water. Then, (i) tetraethoxysilane, $Si(OC_2H_5)_4$ (≥ 99.0 %, Sigma Aldrich) or (ii) Aerosil® 200 fumed SiO_2 (>99.8 %, Evonik Industries) was added as a SiO_2 precursor to the mixture in order to obtain the oxide $(Al_2O_3)_{0.84}(SiO_2)_{0.16}$ stoichiometry. Firstly, urea was dissolved in nitric acid by vigorously stirring using a Ultra-Turrax® (T-25 Basic, IKA) at 6 500 rpm, with a urea:nitric acid solution ratio of 1:5 (m:v). After dissolution, the SiO_2 precursor was added to the solution until total hydrolysis (for tetraethoxysilane) or total dispersion (for fumed silica) was achieved. Next, Disperal® P2 was progressively added with a ratio Disperal®:nitric acid solution of 2:5 (m:v) with stirring speed increased up to 21 500 rpm to ensure total dispersion, leading to a white cloudy sol exempt of visible particles or aggregates. The mixture was left 30 min aging by stirring before washcoating. The washcoat produced with tetraethoxysilane will be further referred to as DUS 1 whereas the one with fumed silica will be referred as DUS 2.

2.1.2. Washcoating procedure

Prior to washcoating, the cordierite, alumina and silicon nitride monoliths were dipped in a concentrated (70 %) nitric acid and magnesia in concentrated sodium hydroxide (~30 %) solution in deionized water for 1 h and subsequently washed thoroughly with hot deionized water. They were dried in a furnace at 300 °C for one hour with a heating ramp of 5 °C min^{-1} in air. The monoliths were then dipped into the aged sol (see 2.1.1) in individual 10 mL glass vial for various durations, ranging from 1 min to 1 h, depending on the monolith chemical nature and geometry. During washcoating, sol viscosity was monitored using a smart series viscosimeter (Fungilab) equipped with an LCP probe. After dipping, the monoliths were removed and blown under a gentle inert gas stream. They were left overnight for aging. The so-obtained matured monoliths were dried in a furnace at 120 °C for 1 h and calcined at 500 °C for 2 h with heating ramps of 1 °C min^{-1} in air. The whole procedure (except for alkali or acid washing) was repeated (when needed) to achieve a washcoat loading of about 10-15 wt-% of the washcoated monolith. The remaining sol was kept aging until gelation occurred. The beaker was placed into a heat chamber at 120 °C for 48 h to ensure solvent elimination before grinding and sieving between 250 and 100 μm to obtain powdered washcoating material.

2.2. Catalyst synthesis

Catalysts were prepared by impregnation with solvent excess onto both the washcoated monoliths and powdered washcoating material. Hexachloroplatinic acid, H_2PtCl_6 (29.79 % solution, Johnson Matthey) and copper nitrate hexahydrate, $Cu(NO_3)_2 \cdot 6 H_2O$ (99.999 %, Sigma Aldrich) were used as metal precursors. Mono- or bimetallic solutions were prepared with the adequate concentration in order to obtain a catalyst with metal loading of 5, 10 or 15 % ($m_{metal} / m_{metal} + m_{support}$). The powders were left to impregnate overnight while stirring at 250 rpm before their transfer into a sand bath heated at 60 °C for solvent evaporation. The obtained powders were kept in a heat chamber at 120 °C for 12 h to improve drying. A calcination treatment was performed in a quartz reactor under an O_2/Ar

stream (Alphagaz 2, Air Liquide) at 200 and 400 °C for 1 and 2 h, followed by a reduction treatment under H_2/Ar at 400 and 800 °C for 1 and 2 h. The powder thus obtained was then sieved between 100 and 250 µm.

2.3. Propellants preparation

LMP-103S and FLP-106 were prepared according to their detailed composition [5] by additive weighing using a laboratory scale (0.1 mg weighing accuracy). Prior to preparation, ammonium dinitramide, $NH_4N(NO_2)_2$ (crystalline >99 %, Eurenco Bofors) was dried at 55 °C for 4 h. LMP-103S was prepared by adding ADN, methanol (HPLC grade 99.99 %, Fisher Scientific) and aqueous ammonia (Analytical Reagent 25.8 wt-% NH_3, Fisher Scientific) in the recommended proportions. FLP-106 preparation was carried out the same way, substituting water (ACS reagent, Sigma Aldrich) and *N*-methylformamide, (99 %, Sigma Aldrich) for aqueous ammonia and methanol. The obtained mixtures were hand-stirred until complete dissolution and room temperature was reached. They were filtered through PTFE hydrophilic filters with 0.45 µm pores (HPF Millex, Merck), leading to yellow and clear solutions.

2.4. Catalytic activity measurement

A constant volume homemade batch reactor (172.5 mL, stainless steel AISI-316L)[12] was used to assess the catalytic decomposition of propellant upon heating. Temperature and pressure were monitored over time. The temperature was recorded with K-type thermocouples (0.5 mm) inside the catalytic bed and inside the reactor, and pressure with a PAA-23 pressure gauge (Keller) in the 0-2 bar (absolute) range. An argon feeding line was connected to the reactor for inert gas flow and evacuation was carried out by an independent line. The catalytic tests were conducted with 80 mg of catalyst and 50 µL of propellant deposited inside a crucible. Acquisition was performed with a Netdaq 2645A interface (Fluke Company) connected to a computer with a LabView virtual instrument. The reactor was purged under argon at 60 mL min^{-1} for 1 h prior to propellant injection which was performed with a microsyringe (100 µL, Hamilton). The heating rate was set to 10 °C min^{-1}. Catalyst tested using this batch reactor were those synthesized from the powdered washcoating material due to crucible volume limitations making it difficult to test monolithic catalyst.

2.5. Characterisation

The specific surface area (SSA) was determined by N_2 adsorption measurements at 77 K using a Micromeritics Tristar 3000 apparatus, following the Brunauer, Emmett and Teller (BET) method. The porous volume was assessed from the isotherm. Prior to analysis, samples were degassed at 250 °C for 8 h. A mercury porosimeter Autopore IV (Micromeritics) was used to assess the specific surface area of the monoliths.

X-ray powder diffractograms were recorded at ambient temperature using a D5005 θ-θ Brucker diffractometer equipped with a back-monochromatized source of Cu Kα radiation (λ(Kα$_1$)) = 0.15406 nm). The diffractograms were acquired in the 5-90 ° (2 θ) range, with a 0.01 ° (2 θ) step size and a dwell time of 1 s per step, with the sample rotating at 30 rpm.

Elemental analyses were performed using inductively coupled plasma optical emission spectrometry (ICP-OES) by mean of a Perkin Elmer Optima 2000 DV apparatus. The samples were mineralised in a mixture of nitric, hydrochloric and hydrofluoric acid in an Anton Paar microwave oven.

The monoliths were inspected using a scanning electron microscope SEM-FEG 7001F-TTLS from JEOL.

3. Results and discussion

3.1. Monoliths textural and structural properties

The α-Al_2O_3, MgO and Si_3N_4 monoliths manifest a perfect crystalline profile, as displayed on the XRD patterns shown in Figure 3. That means that no phase transition is expected after additional heat treatment, as well as no massive shrinkage, which is in agreement with their sintering temperatures (1 650, 1 550, 1 780 °C, respectively). The diffraction peaks correspond to the reference powder diffraction files (ICDD code 00-046-1212 for Al_2O_3, 00-045-0946 for MgO and 00-033-1160 for Si_3N_4). Some reflexions in the alumina and silicon nitride samples cannot been attributed to their crystalline state. They are believed to originate from impurities, but not have any significant influence on the monolith mechanical or chemical properties toward washcoating. However, cordierite monoliths do not have a perfectly crystallised profile. This could be due to their lower sintering temperature (1 300 °C).
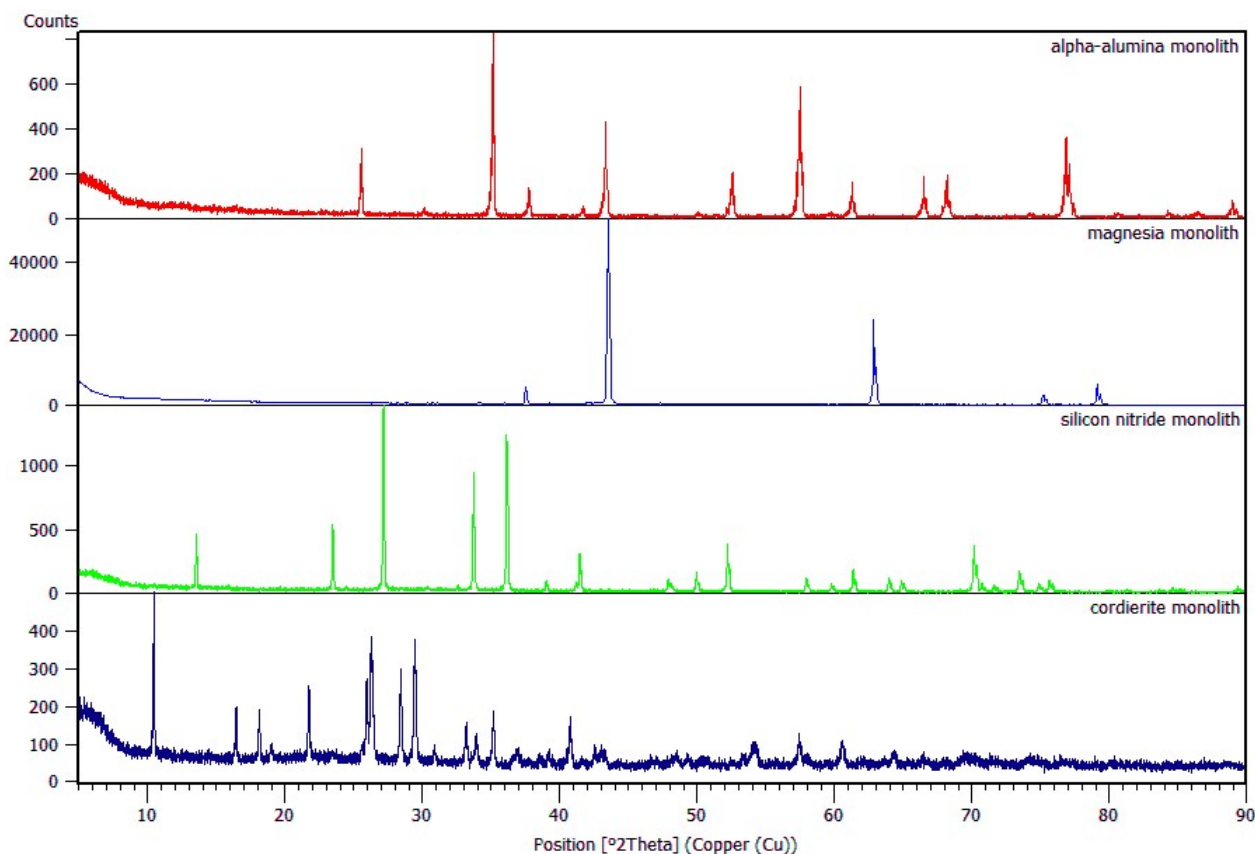
Figure 3. X-ray diffraction profiles for monoliths as received

Monoliths samples had to be cut in 4 quarters along the central axis of the cylinder in order to fit in the sorptiometer analysis cells. A diamond-studded saw was used for this purpose. Whole monoliths were used for the mercury porosimetry. Results are displayed in Table 3. Silicon nitride monoliths were not analysed due to the limited amount of samples.

Table 3. Specific Surface Area (a) obtained from nitrogen sorptiometry (BET), mercury porosimetry (Hg) and pore diameter ($\varnothing$) results for the crude monoliths

Monolith chemical nature[a]	a / m^2 g^{-1} (BET)	a / m^2 g^{-1} (Hg)	$\varnothing$ / μm
α-Alumina	0	0	61.8
Cordierite	<0.01	0.24	3.06
Magnesia	<0.01	0.32	1.52

Monoliths by themselves do not exhibit meso- or microporosity, which is confirmed by the low SSA value. They do, however, exhibit some macroporosity. Thus, a washcoating step is necessary in order to deposit a second, porous support having high surface area which will promote a good dispersion of the active phase allowing better contact with propellant.

3.2. Monoliths behaviour towards washcoating

Table 4 gathers the results collected from several washcoating mass analyses conducted on monoliths. The layer deposition on alumina monoliths with triangular channel did not succeed, with values lower than 1 %, even when changing the SiO_2 precursor, leading to a brittle and crumbled powder after calcination. This can be explained by the very smooth surface and absence of any porosity as shown in Figure 3, which prevents washcoat adherence. The polyhedral and cellular monoliths, though displaying a mean gain of 4.75 %, did not present a satisfying texture or deposition quality. It was observed that after maturation pieces of washcoat moved to the bottom, leading to chunks trapped between the struts.

Maleix *et al.*

Table 4. Washcoating results on different monolithic samples

Sample	Nature	Geometry	m_i	$m_{cleaned}$	Δm	Washcoat nature	m_{coated}	$m_{washcoat}$	Washcoat $\%_{wt}$
A-01			2,9401	2,9399	-0,0002		2,9581	0,0182	0.6
A-02		triangular	2,9471	2,9472	0,0001		2,9687	0,0215	0.7
A-03			2,9688	2,9688	0,0000	DUS 1	2,9926	0,0238	0.8
A-C03	α-alumina	cellular	1,0649	1,0647	-0,0002		1,1171	0,0524	4.7
A-P03		polyhedral	1,7384	1,7386	0,0002		1,8254	0,0868	4.8
A23-06		triangular	2,8289	2,8289	0,0000	DUS 2	2,8325	0,0036	0.1
A23-07			2,8372	2,8371	-0,0001		2,8424	0,0053	0.2
C856-01			1.2986	1.2984	-0.0002		1.5843	0.2859	18.0
C856-02		triangular	1.4324	1.4322	-0.0002		1.6755	0.2433	14.5
C856-03			1.4317	1.4313	-0.0004		1.7166	0.2853	16.6
C856-C03	Cordierite	cellular	0.5566	0.5563	-0.0003	DUS 1	0.6604	0.1041	15.8
C856-C04			0.5612	0.5612	0.0000		0.6534	0.0922	14.1
C856-P04		polyhedral	0.7929	0.7930	0.0001		1.0388	0.2458	23.7
C856-P05			0.8048	0.8046	-0.0002		1.0428	0.2382	22.8
SN-10144-02	Silicon nitride	triangular	1.4204	1.4195	-0.0009		1.5398	0.1203	7.8
M-17		triangular	1.4576	1.4568	-0.0008	DUS 1	1.6553	0.1985	12.0
M-18		triangular	1.5267	1.5297	0.0030		1.7260	0.1963	11.4
M17-T02	Magnesia	triangular	1.4651	1.4649	-0.0002		1.5317	0.0668	4.4
M13-P01		polyhedral	0.7700	0.7687	-0.0013	DUS 2	0.9831	0.2144	21.8
M13-D01		tetrahedral	0.7501	0.7539	0.0038		0.8822	0.1283	14.5

The washcoat layer was well deposited onto the cordierite monoliths, as shown in Figure 4. A few peripheral channels were clogged during the process, attributed to the blowing method. But the deposited material presented a very smooth and quite homogeneous surface as can be seen in Figure 5. The mass increase due to washcoat ranged from 14 to 18 wt.% for triangular and cellular geometry, and 23-24 wt% for the polyhedral geometry. This variation suffered the same issue as alumina polyhedral monoliths, where the washcoat moved to the bottom during maturation. This behaviour could partially be explained by the smaller geometric surface of the polyhedral struts compared to triangular ones. The layer thickness was estimated to be about 50 µm for the triangular geometry.
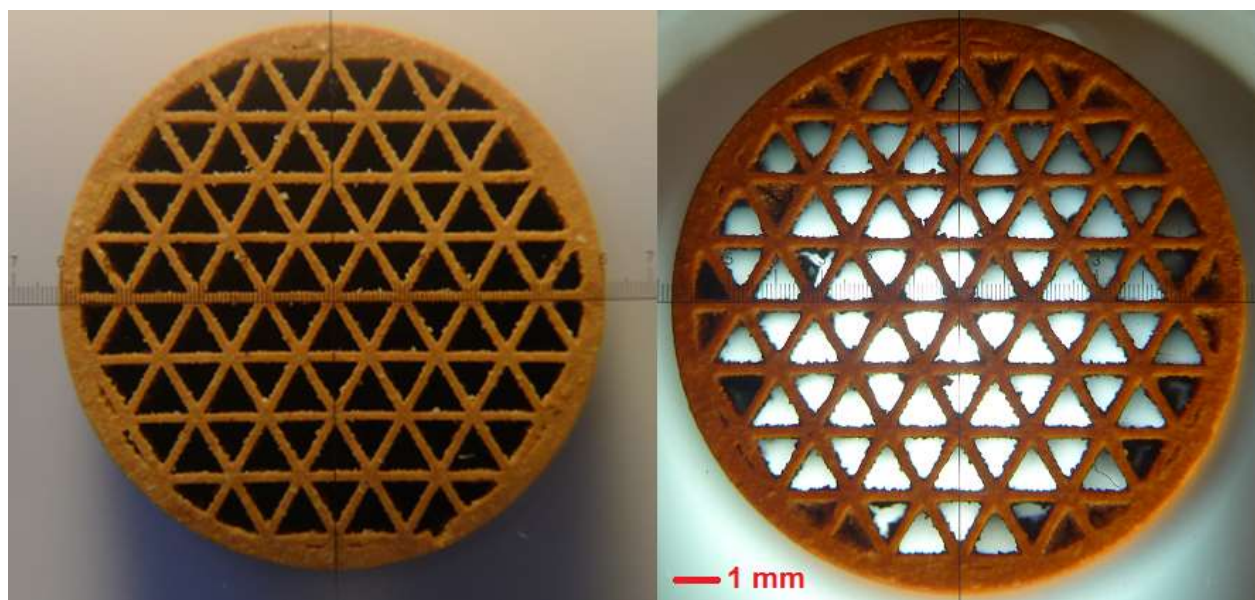

Figure 4. Magnification of a cordierite monolith before (left) and after (right) washcoating with DUS 1 sol
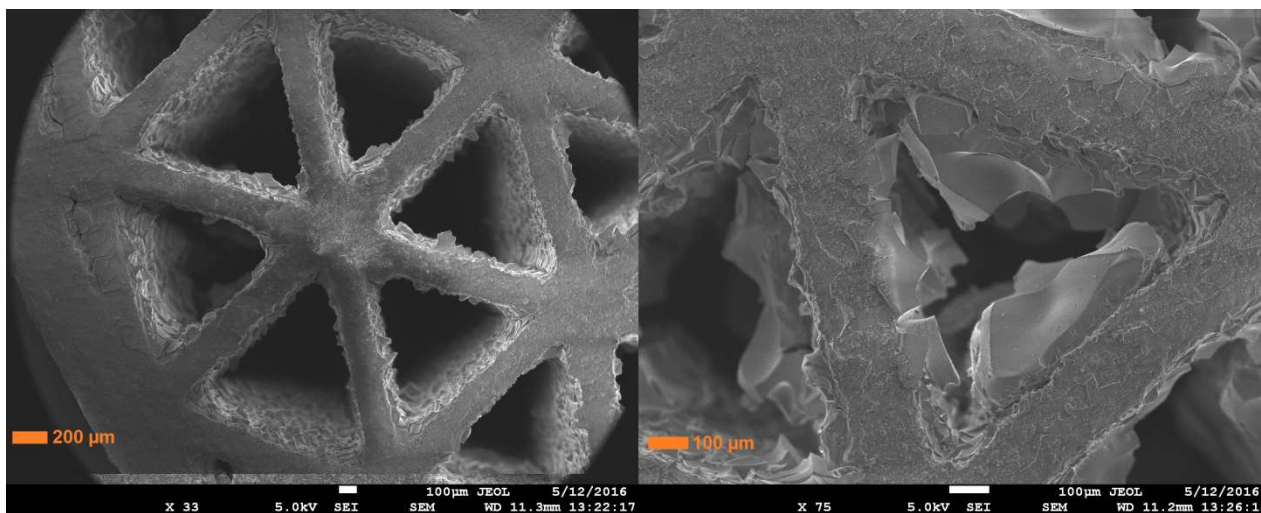
Figure 5. SEM picture of a cordierite monolith with homogeneous deposition (left) and example of clogged channel (right)

The magnesia monoliths, despite presenting a mass gain of 11-12 % with the DUS 1 washcoat did however present a non-homogeneous layer, both in thickness and covering, as shown in optical photographs of magnesia substrates displayed in Figure 6. An anomalous gelation occurred a few minutes after monolith soaking, leading to a partial clogging and cracks distributed on the external wall and on the cylinder sides. This phenomenon is considered to be caused by a surface reaction between tetraethoxysilane and magnesium atoms, forming magnesium ethoxide which results in a hindered anchorage of the porous layer.
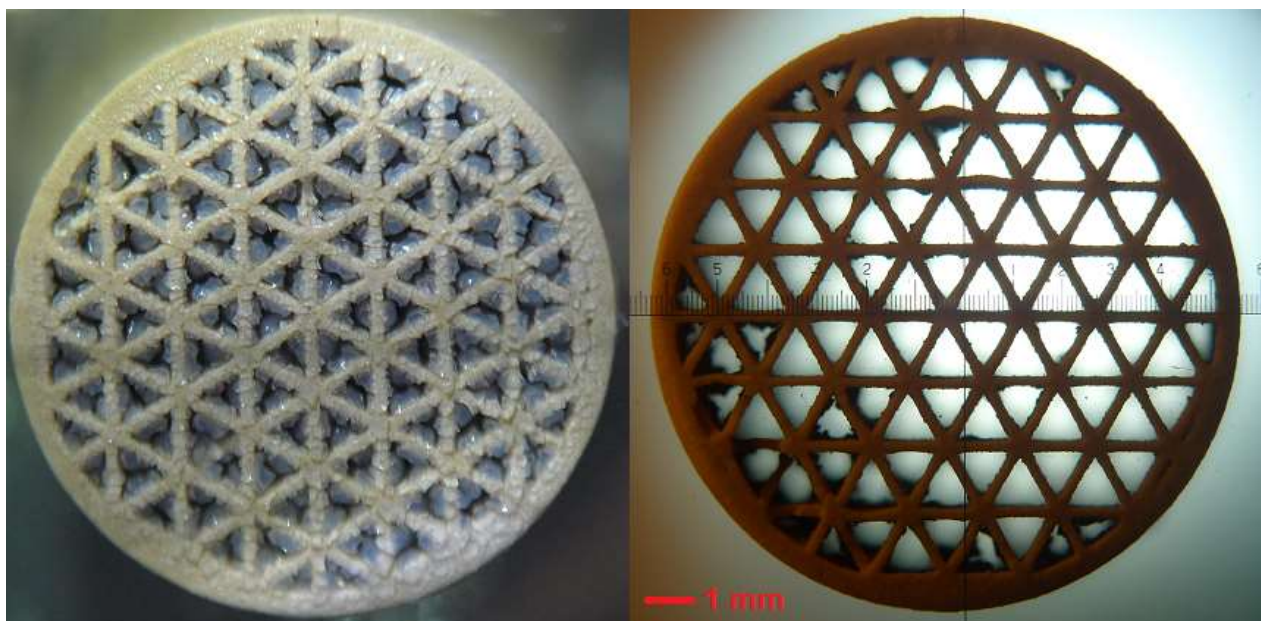

Figure 6. Magnification of a MgO monolith with DUS 1 (left) and DUS 2 (right) washcoat layer. Same coating time and sol viscosity

Changing the washcoating procedure (substituting tetraethoxysilane by fumed silica) improved the washcoating with a more homogeneous thickness and without embrittling the external walls. The mass gain was nonetheless only about 4 %. The diamond structure was investigated using SEM, as shown in Figure 7. The layer thickness was estimated to about 30 µm.
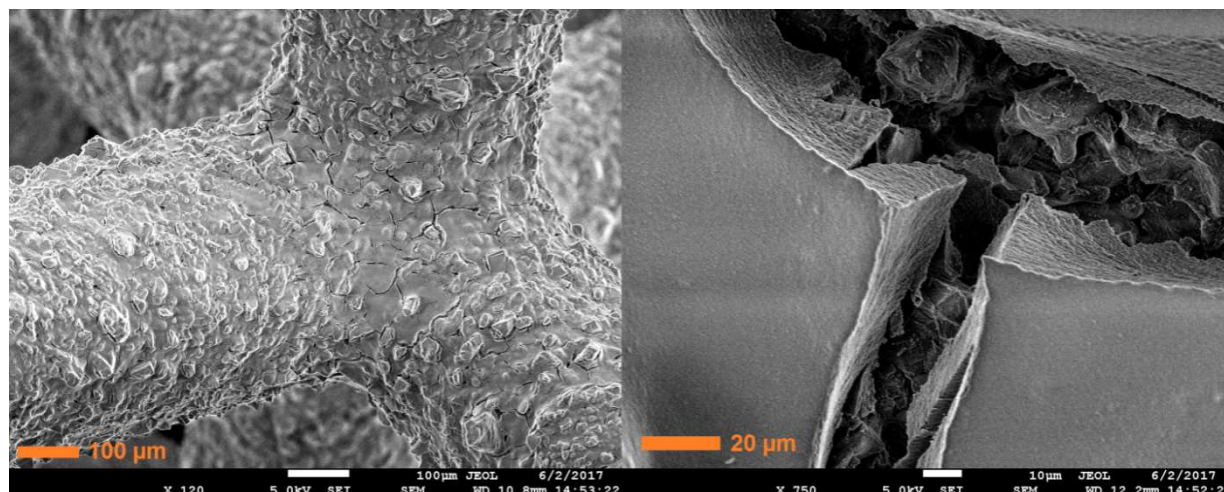
Figure 7. SEM picture of a diamond MgO monolith coated with DUS 2 sol

3.3. Evolution of the washcoating material vs. high temperature heat treatment

The washcoat recovered after the synthesis (see section 2.1.1) was subjected to several heat treatments in order to assess the specific surface area evolution and the crystallization profile. This is detailed in the following subsection.

3.3.1. Textural properties

The SSA evolution of DUS1 and 2 washcoats subjected to different heat treatments are presented in Table 5 where temperature and time of the treatments are detailed. The specific surface area of both supports decreases as the temperature treatment increases. This is characteristic for the gamma-to-alpha alumina phase transition. However, the addition of silicon as a doping agent seems to preserve a good surface area, despite the treatment duration. This matches with the work of McArdle *et al.* [13], were boehmite precursor crystallise totally into α-Al$_2$O$_3$ with a specific area of less than 10 m^2 g^{-1} without any crystallization retardant. It is also important to note that the effective treatment time is higher as calcination temperature increases, since more time is necessary to reach the threshold temperature, and more time is needed to cool-down the furnace. As an example, there is 1 h difference between a treatment at 1200 °C and 1500 °C under the same heating and cooling conditions.

Table 5. SSA evolution of the powdered DUS washcoat material for different heat treatments

Material	SSA (m^2 g^{-1}, BET) evolution after thermal treatment						
	4 h				**2 h**	**3 min**	**10 min**
	500 °C	1 200 °C	1 350 °C	1 500 °C	1 600 °C	1 500 °C	
DUS 1	379	91	9	3	<0.1	/	8
DUS 2	279	85	8	3	<0.1	107	10

Further tests were conducted with a heating apparatus allowing the quick introduction and removal of a sample into a vertical furnace preheated at 1 500 °C so that high temperature gradients can be simulated (1 500 °C within a few seconds). DUS 2 powder thus introduced for 3 min at 1 500 °C suffered from a sintering leading to a decrease of SSA from 107 m^2 g^{-1} to 10 m^2 g^{-1} after 10 min.

3.3.2. Structural properties

The X-ray diffraction profiles for DUS1 powder calcined at different temperatures for 4 h are depicted in Figure 8. At low temperatures (500 or 1 200 °C), no reflections could be exclusively assigned to boehmite (γ-AlO(OH)), alumina, silica or mullite (x Al$_2$O$_3$-y SiO$_2$). The amorphous structures account for the high specific surface area, even at 1 200 °C. As the temperature increases, the powder crystallised much more, leading to peaks ascribed to both stoichiometric mullite (Al$_2$SiO$_5$) and α-alumina, which is in excess according to the synthesis conditions. The loss of specific surface area is explained by the phase transition at 1 350 °C. Figure 9 compares DUS1 diffraction pattern

DEVELOPMENT OF CATALYTIC MATERIALS FOR DECOMPOSITION OF ADN-BASED MONOPROPELLANTS

with DUS2 after heat treatments at 1200 and 1500 °C. It illustrates that the two washcoating procedures lead to the same material before and after high temperature treatment.
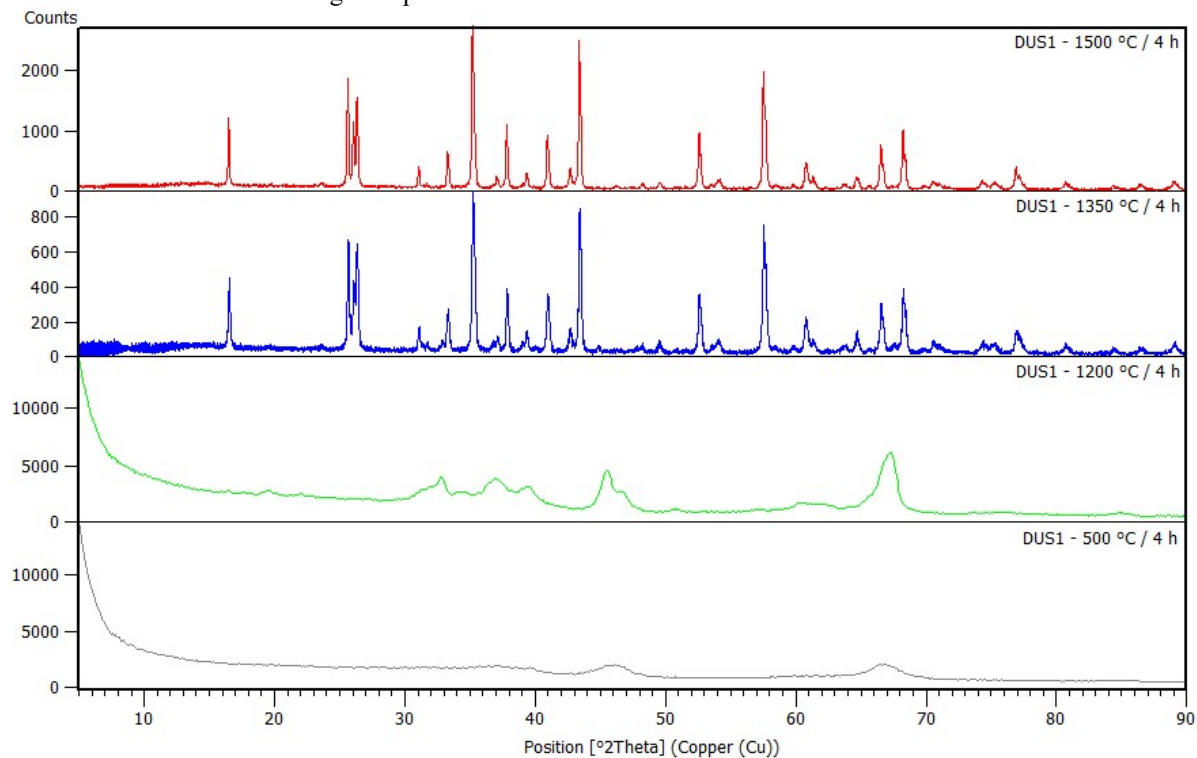

Figure 8. X-ray diffraction profile for the DUS 1 powder after treatment at 500, 1 200, 1 350 and 1 500 °C (bottom to top)
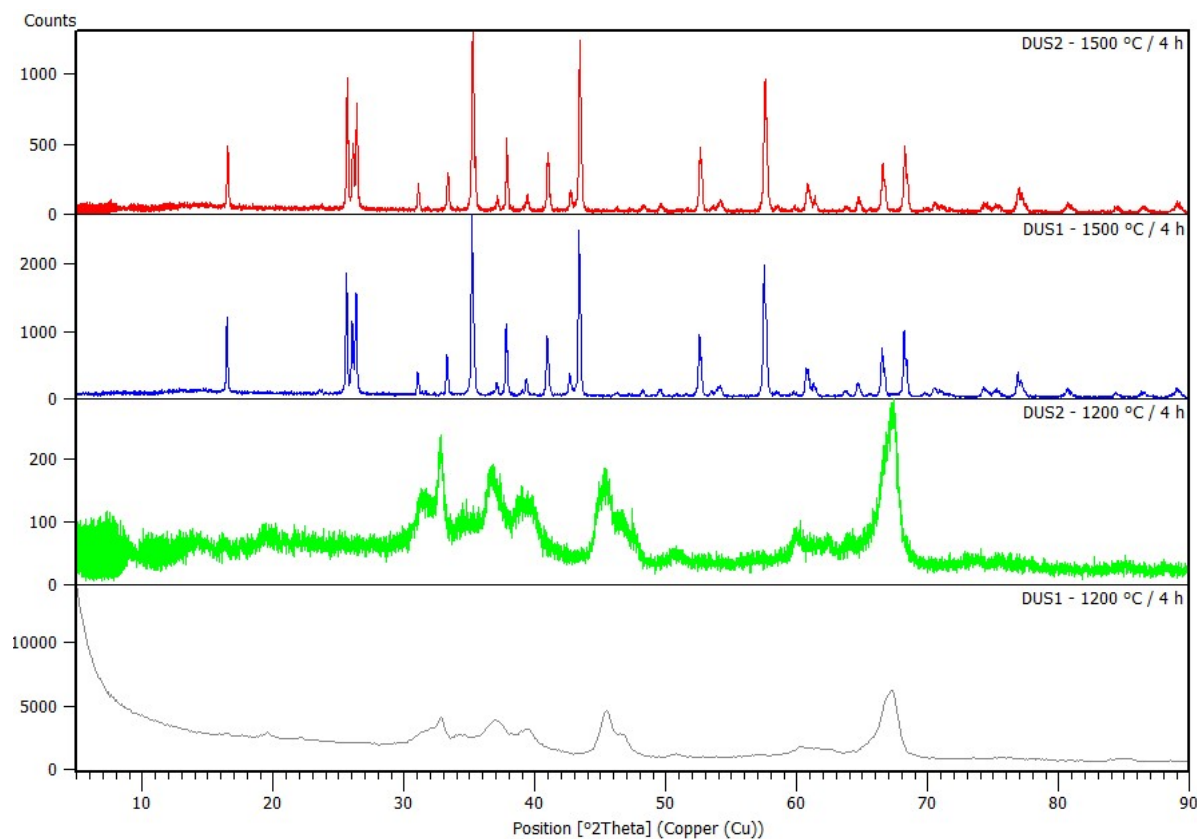

Figure 9. X-ray diffraction profile comparison for DUS 2 & 1 treated at 1 500 °C and at 500 °C for 4 h (from top to bottom)

9

3.4. Catalytic activity toward the decomposition of propellants

Figure 10 shows an example of temperature and pressure profile obtained after a catalytic test. The following studied parameters are determined:

- The decomposition temperature (T_{dec})
- The maximum temperature reached during the decomposition (T_{max})
- The temperature difference between T_{max} & T_{dec} (ΔT)
- The pressure difference between the pressure prior to decomposition and $\underline{P}_{max}$ (ΔP_{max})
- The final pressure difference corresponding to the gas generated by the propellant decomposition (ΔP)
- The temperature (s_t) and pressure (s_t) rate between T_{dec} and T_{max} defining the rising slope
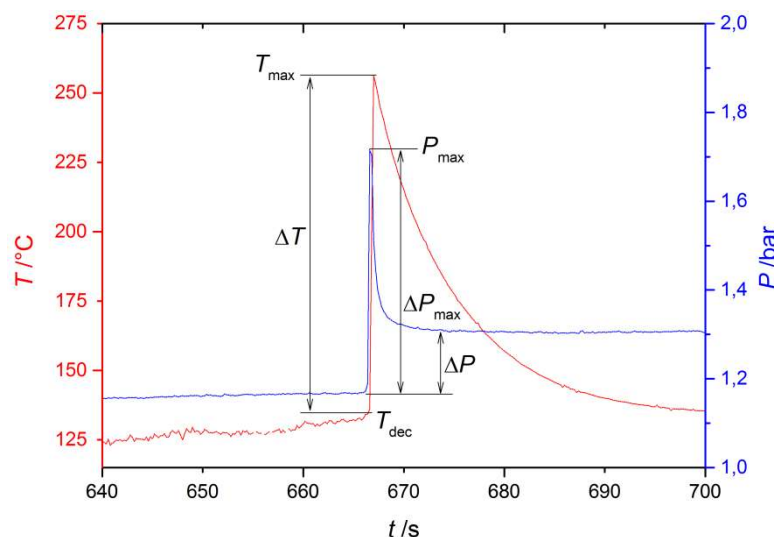

Figure 10. Example of a temperature and pressure record vs. time during propellant decomposition in the batch reactor

Test results for three catalysts (Pt/DUS1, Cu/DUS1 and Pt-Cu/DUS1) are gathered in Table 6. Tests were performed on powder calcined at 500 °C. In the absence of a catalyst, that is with the non-impregnated washcoat, LMP-103S decomposes at 134 °C, which is a temperature lower than FLP-106 which decomposes at 148 °C. Ammonia and methanol are much more volatile than N¬methylformamide, so that ADN decomposes more easily. However, it displays, a lower T_{max} and slower decomposition kinetics, embodied by S_T value. Numerous metals have been tested to tentatively lower the decomposition temperature of the different ADN-based blends, namely platinum group metals and mainly Cu in the CuO form as transition metal. Results show that Pt, as well as Cu, have a strong catalytic activity towards ADN blends, since the decomposition temperature for FLP-106 decreases from 148 to 116 °C with Pt and from 148 to 135 °C with Cu. Decomposition temperature of LMP-103S decreases from 134 to 110 °C with Pt and to 102 °C with Cu. The combination of the two metals leads to the best temperature decrease, about 50 °C for FLP-106 and 30 °C for LMP-103S, which are better than the temperatures previously reported [9]. Tests conducted with the DUS powder calcined at 1200 °C decreased the temperature of 40 and 20 °C for FLP-106 and LMP-103S, which corresponds to an activity loss of 25 and 50 %, respectively, which is attributed to the specific surface area loss during the heating process.

Table 6. Results for catalytic decomposition of FLP-106 and LMP-103S

	FLP-106					LMP-103S				
	thermal[a]	Pt-10[b]	Cu-10[b]	Pt-Cu	Pt-Cu[c]	thermal[a]	Pt-10[b]	Cu-10[b]	Pt-Cu	Pt-Cu[c]
T_{dec} / °C	148	116	135	97	104	134	110	102	105	115
T_{max} /°C	330	388	256	266	192	281	345	219	292	219
ΔT / °C	182	272	121	169	88	147	235	117	187	104
S_T / °C s^{-1}	91	170	30	140	88	53	90	10	64	260
ΔP_{max}/ bar	0.24	0.55	0.24	0.18	0.37	0.15	0.63	0.08	0.64	0.40
ΔP / bar	0.03	0.10	0.14	0.10	0.09	0.06	0.08	0.06	0.06	0.06
S_P / bar s^{-1}	0.24	0.55	0.06	0.35	0.37	0.07	1.57	< 0.01	3.20	2

[a]Test conducted with the crude washcoat without active phase
[b]Active phase loading of 10 wt.%, confirmed by ICP-OES

^{c}Washcoat calcined at 1 200 °C

4. Conclusion

New monoliths with unprecedented 3D geometry, impossible to obtain by conventional extrusion means, were coated using a sol-gel method. Two distinctive processes have been developed, adapted to the chemical nature of the monoliths, consisting in the addition of silicon-doped alumina layer. The viscosity parameters were adjusted in order to get the most homogeneous and the least friable layer possible. The α-alumina monoliths exhibit a smooth and non-porous surface, therefore the coating could not be applied to an acceptable degree. On the other hand, the magnesia and cordierite monoliths led to coating deposits of 5 to 15 wt-% average weight depending on their geometries, turning them suitable for the use as catalyst supports.

Textural properties of the coatings have been studied in relation to different thermal treatments of various durations. A particular porosity could be maintained for an extensive time at 1200 °C and for a shortened time at 1500 °C. Coatings could be used for applications in which the steady state adiabatic decomposition temperature of the propellant does not exceed 1 200 °C, or even for applications which work in few second pulse mode for a temperature close to or slightly higher than 1 500 °C.

Despite the several active phases which were tested, this work presents only the ones having the best activity regarding the FLP-106 and LMP-103S decomposition. The best results were achieved for a bimetallic catalyst with precise proportions of platinum-copper, which resulted in the lowering of the ignition temperature of 50 °C for FLP-106 and of 30 °C for LMP-103S.

Acknowledgement

References

[1] Schmidt, E.W. History of Hydrazine Monopropellants. Presented at: AIAA pacific Northwest Section Young Professionals Technical Symposium. Seattle. 2009.

[2] Sackheim, R. L. & Masse, R. K. 2014. Green Propulsion Advancement: Challenging the Maturity of Monopropellant Hydrazine. J. Prop. Power 30: 265–276.

[3] Valencia-Bel, F & Smith M. Replacement of Conventional Spacecraft Propellants with Green Propellants. Space propulsion 2012, Bordeaux.

[4] Rheform Project website, Available at: www.rheform-h2020.eu

[5] Gohardani, A. S. *et al.* 2014.Green space propulsion: Opportunities and prospects. Progress in Aerospace Sciences 71: 128–149.

[6] Anflo, K. & Crowe, B. In-Space Demonstration of an ADN-based Propulsion System. In *47th* AIAA/ASME/SAE/ASEE Joint Propulsion Conference & Exhibit, San Diego, California, 2011-5832, 2011

[7] Schwentenwein, M. & Homa, J. 2015. Additive Manufacturing of Dense Alumina Ceramics. Int. J. Appl. Ceram. Technol. 12: 1–7.

[8] Nijhuis, T.A. Kreutzer, M.T. Romijn, A.C.J. Kapteijn, F. Moulijn, J.A.. 2001. Monolithic catalysts as efficient three-phase reactors. Chem. Eng. Sci. 56: 823–829.

[9] Batonneau, Y. et al. 2013. Green Propulsion: Catalysts for the European FP7 Project GRASP. Top Catal 57: 656–667.

[10] Courtheoux, L., Gautron, E., Rossignol, S. & Kappenstein, C. 2005. Transformation of platinum supported on silicon-doped alumina during the catalytic decomposition of energetic ionic liquid. J. Catal. 232: 10–18.

[11] Structured Catalysts and Reactors, 2nded., Andrzej Cybulski & Jacob A. Moulijn, CRC Press 2005

[12] Eloirdi, R., Rossignol S., Kappenstein C., Duprez, D. and Pillet, N. 2003. Monopropellant decomposition catalysts. III. Design and use of a batch reactor for catalytic decomposition of different monopropellants, J. Prop. and Power. 19:213-219.

[13] McArdle, J. L. & Messing, G. L. 1993. Transformation, Microstructure Development, and Densification in alpha-Fe_2O_3-Seeded Boehmite-Derived Alumina. J. Am. Ceram. Soc. 76: 214–222.

[14] Gronland, T.A., Westerberg, B., Bergman, G., Anflo, K., Brand, J., Lyckfeldt, O., Agrell, J., Ersson, A., Järas, S., Boutonnet, M., Wingborg, N., European Patent N° EP 1 389 271 B1.

[15] Korobeinichev, O. P., Paletsky, A. A., Tereschenko, A. G. & Volkov, E. N. 2002. Combustion of ammonium dinitramide/polycaprolactone propellants. Proc. Comb.Inst. 29: 2955–2961.